Chemistry–A European Journal

Research Article
doi.org/10.1002/chem.202202493

Chemistry Europe
European Chemical Societies Publishing

www.chemeurj.org

Activation of Ge–H and Sn–H Bonds with N-Heterocyclic Carbenes and a Cyclic (Alkyl)(amino)carbene

Michael S. M. Philipp,[a] Rüdiger Bertermann,[a] and Udo Radius*[a]

Abstract: A study of the reactivity of several N-heterocyclic carbenes (NHCs) and the cyclic (alkyl)(amino)carbene 1-(2,6-di-*iso*-propylphenyl)-3,3,5,5-tetramethyl-pyrrolidin-2-ylidene (cAAC^{Me}) with the group 14 hydrides GeH_2Mes_2 and SnH_2Me_2 (Me = CH_3, Mes = 1,3,5-$(CH_3)_3C_6H_2$) is presented. The reaction of GeH_2Mes_2 with cAAC^{Me} led to the insertion of cAAC^{Me} into one Ge–H bond to give cAAC^{Me}H–$GeHMes_2$ (**1**). If 1,3,4,5-tetramethyl-imidazolin-2-ylidene (Me_2Im^{Me}) was used as the carbene, NHC-mediated dehydrogenative coupling occurred, which led to the NHC-stabilized germylene Me_2Im^{Me}·$GeMes_2$ (**2**). The reaction of SnH_2Me_2 with cAAC^{Me} also afforded the insertion product cAAC^{Me}H–$SnHMe_2$ (**3**), and reaction of two equivalents Me_2Im^{Me} with SnH_2Me_2 gave the NHC-stabilized stannylene Me_2Im^{Me}·$SnMe_2$ (**4**). If the sterically more demanding NHCs Me_2Im^{Me}, 1,3-di-*iso*propyl-4,5-dimethyl-imidazolin-2-ylidene (iPr_2Im^{Me}) and 1,3-bis-(2,6-di-*iso*propylphenyl)-imidazolin-2-ylidene ($Dipp_2Im$) were employed, selective formation of cyclic oligomers $(SnMe_2)_n$ (**5**; n = 5–8) in high yield was observed. These cyclic oligomers were also obtained from the controlled decomposition of cAAC^{Me}H–$SnHMe_2$ (**3**).

Introduction

N-heterocyclic carbenes (NHCs)[1] and the related cyclic (alkyl)(amino)carbenes (cAACs)[1,2] are first-class ligands for a large variety of molecules and afforded reactivities in main group element chemistry that would not be feasible without this particular ligand support. Their electronic and steric properties can be precisely adjusted depending on the substitution pattern of the carbene.[3] Our group has been working on the synthesis and the reactivity of various carbene-stabilized compounds of main-group elements in recent years,[4] including the reactivity of NHCs towards several group 14 compounds.[5]

This work originates from our previous studies on the reactivity of group 14 element hydrides with different NHCs.[5a,b,d] We demonstrated earlier that NHCs react with the silicon hydrides SiH_3Ph, SiH_2Ph_2 and $SiHPh_3$ with insertion of silylene moieties into the C–N bond of the NHCs, which leads to ring expansion (RER = ring expansion reaction) of the NHC and formation of diaza-silinanes **A**–**C** (Scheme 1).[5a] RERs were feasible using primary, secondary and tertiary silanes $Ph_{4-n}SiH_n$ and a variety of NHCs, that is, saturated and unsaturated NHCs with N-alkyl and N-aryl substituents. In the meantime, we[4a,b,d–f,5a,6] and others (for the elements Be,[7] B,[8] Al[8g,9] and Si[10]) demonstrated that RERs are a rather general processes in NHC main group chemistry. The products isolated are typically six-membered heterocycles which were formed by C–N bond cleavage within the NHC, migration of two hydrogen atoms to the (former) NHC carbene carbon atom and formal insertion of a subvalent (e.g., a silylene) moiety into the C–N bond. For the reaction of Ph_3SiH even migration of a phenyl group was observed.[5a]

Bertrand and co-workers reported prior to our work the insertion of cAAC^{Cy} (cAAC^{Cy} = 2-azaspiro[4.5]dec-2-(2,6-diisopropylphenyl)-3,3-dimethyl-1-ylidene) into the Si–H bond of different silanes leading to stable cAAC insertion products, for example cAAC^{Cy}H–$SiHPh_2$ from the equimolar reaction of cAAC^{Cy} with SiH_2Ph_2.[11]

For the reaction of the NHCs iPr_2Im (1,3-di-*iso*-propylimidazolin-2-ylidene) and iPr_2Im^{Me} (1,3-di-*iso*-propyl-4,5-dimethyl-imidazolin-2-ylidene) with the higher homologue $SnHPh_3$, a completely different reaction pathway was observed, which led not to $SnAr_2$ insertion but to NHC-mediated dehydrogenative coupling (DHC) of the stannane with formation of the hexaaryl distannane Ph_6Sn_2 **D** and the aminal $NHCH_2$ (Scheme 1).[5d] We[5d,12] and others[13] demonstrated that NHCs are very good hydrogen acceptors and that NHC-mediated DHC may be used on a preparative scale for element element bond formation, for example for the synthesis of NHC–phosphinidene adducts, for diphosphines and cyclic oligophosphines.[12]

Wesemann and co-workers exploited NHC-mediated DHC in tin chemistry rather systematically and demonstrated in their work that the reaction of the diarylstannanes SnH_2Ar_2 (Ar = Ph, Trip; Trip = 2,4,6-triisopropylphenyl) with Et_2Im^{Me} (Et_2Im^{Me} = 1,3-diethyl-4,5-dimethyl-imidazolin-2-ylidene) or Me_2Im^{Me} as the hydrogen acceptor lead to the formation of different reaction products, depending on the tin hydride and the stoichiometry used (Figure 1).

[a] *M. S. M. Philipp, Dr. R. Bertermann, Prof. Dr. U. Radius*
Institute of Inorganic Chemistry
Julius-Maximilians-Universität Würzburg
Am Hubland, 97074 Würzburg (Germany)
E-mail: u.radius@uni-wuerzburg.de
Homepage: http://www.ak-radius.de

Supporting information for this article is available on the WWW under https://doi.org/10.1002/chem.202202493

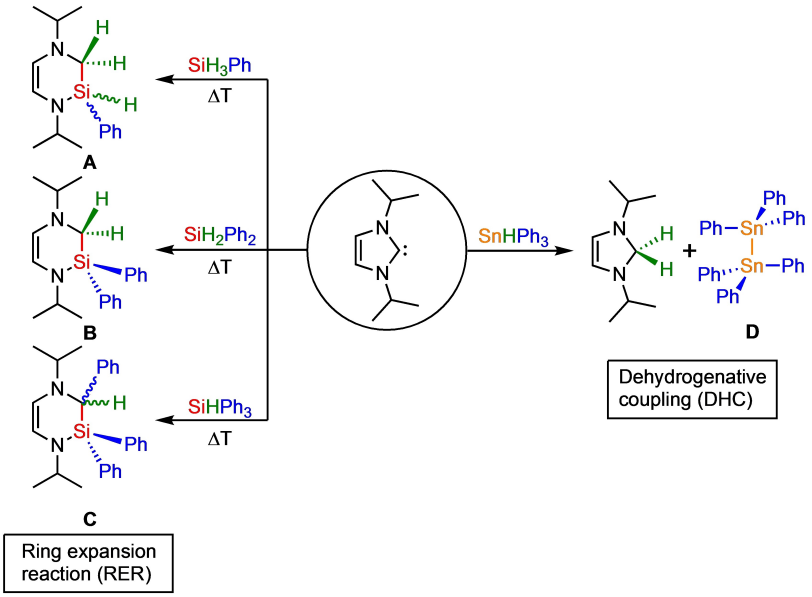

Scheme 1. Previous work from our group on the reactivity of group 14 element hydrides with NHCs (*i*Pr$_2$Im).

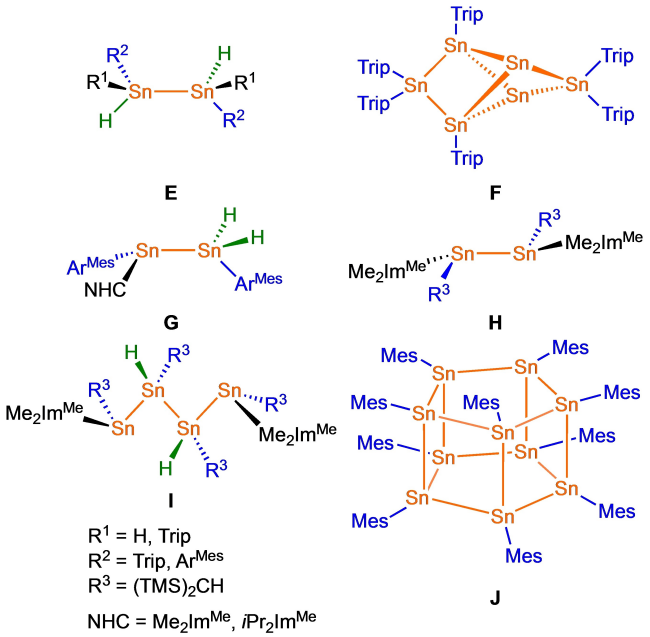

Figure 1. NHC-mediated dehydrogenative Sn–Sn coupling.

Using a 2:1 ratio of SnH_2Trip_2:Et_2Im^{Me}, the tetraorganyl distannane $Sn_2H_2Trip_4$ (Figure 1, **E**; R^1 = Trip,) was obtained from NHC-mediated DHC, whereas from a 1:2 SnH_2Tripp_2/Et_2Im^{Me} ratio, the NHC-stabilized stannylenes Et_2Im^{Me}·$SnAr_2$ (Ar = Ph, Trip) were formed.[14] Similarly, the reaction of Me_2Im^{Me} with SnH_2Trip_2 afforded the NHC-stabilized stannylene Me_2Im^{Me}·$SnTrip_2$.[15] Analogous reactions of the mono-organyl stannane SnH_3Trip with different NHCs (NHC = Et_2Im^{Me}, Me_2Im^{Me}) led to the corresponding NHC-stabilized stannylenes NHC·SnHTrip.[14,16] At a ratio of 1:1.5 (SnH_3Trip/Et_2Im^{Me}), the reaction yielded the interesting tin cluster Sn_6Trip_6 (Figure 1, **F**).[14] Reacting the backbone methylated NHCs Me_2Im^{Me} and iPr_2Im^{Me} (1,3-di-isopropyl-4,5-dimethyl-imidazolin-2-ylidene) with SnH_3Ar^{Mes} (Ar^{Mes} = 2,6-dimesitylphenyl, mesityl = 2,4,6-trimethylphenyl) in a ratio of 1:2 (SnH_3Ar^{Mes}:NHC) afforded the stannylene NHC·$SnHAr^{Mes}$, whereas the stannyl-stannylenes $Ar^{Mes}Sn(NHC)SnH_2Ar^{Mes}$ (Figure 1, **G**) were formed by using a ratio of 1:1.5 (SnH_3Ar^{Mes}/NHC). The latter was exploited for the reaction with another equivalent of $Ar^{Mes}SnH_3$, which gave the distannane $Sn_2H_4Ar^{Mes}{}_2$ (Figure 1, **E**; R^1 = H, R^2 = Ar^{Mes}) with loss of $NHCH_2$.[17] Furthermore, the Me_2Im^{Me}-induced DHC of the mono-organyl stannane SnH_3R (R = $CH(SiMe_3)_2$) offered a wide range of interesting compounds, such as the dialkyl distannyne $R^3{}_2Sn_2(Me_2Im^{Me})_2$ (Figure 1, **H**; R^3 = $CH(SiMe_3)_2$) and the tin chain $(Me_2Im^{Me}{\cdot}SnR^3{-}SnHR^3)_2$ (Figure 1, **I**), depending on the reaction conditions. A very interesting neutral Sn_{10} cluster, $(SnMes)_{10}$ (Figure 1, **J**), was obtained from the Et_2Im^{Me}-mediated DHC of SnH_3Mes.[18] In addition, the NHC-stabilized stannylene iPr_2Im^{Me}·SnHTbb as well as the germylenes Me_2Im^{Me}·GeHR (R = 2,6-$Trip_2C_6H_3$, Trip = 2,4,6-triisopropylphenyl; R = Tbb = 2,6-(CH-$(SiMe_3)_2)_2$-4-(*t*Bu)C_6H_2) were isolated starting from the corresponding stannane or germane EH_3R and an NHC.[19] However, with the latter exception the reactivity of NHCs with respect to germanium hydrides is rather unexplored and mainly restricted on the formation of NHC germanium hydride adducts from the corresponding NHC germanium chloride adducts.[8a,20,21] With respect of our investigations on the RER of silicon hydrides we were interested in the reactivity of NHCs with similar germanium and tin hydrides and report here first results on the reactivity of various carbenes towards hydride compounds of the heavier group 14 elements.

Results and Discussion

Briefly after our report on RER, several groups reported theoretical investigations into the reaction mechanism of the ring expansion, based on our original proposal.[5b,8g, 10b, 22] This mechanism can be in principle divided into four steps, which involve the adduct formation between the Lewis-basic NHC and the Lewis-acidic hydride, the hydride migration from the main group element hydride to the carbene carbon atom, C–N bond cleavage and ring expansion of the NHC with insertion of the main group element unit into the NHC ring, and a potential stabilization of the ring-expanded NHC by migration of substituents or by additional coordination of a Lewis-base, like an NHC. Wilson and Dutton and co-workers presented a theoretical study on the detailed reaction pathway and indicated that formation of C–H bonds is the crucial factor in the over-all transformation, resulting in an exothermic process.[22a] For SiH_2Ph_2 and Me_2Im, the insertion of the NHC into the Si–H bond was calculated to be the rate determining step, associated with a barrier of 113.4 kJ mol^{-1} at the M06-2X/6-31G(d) (optimized geometries)//MP2/TZVP (single-point energy) level of theory. Furthermore, these authors stated that the trends observed in the reaction energetics were largely independent of the method (SCS-MP2, PBE1PBE, M06-2X) and basis set used (6-31G(d), TZVP), with deviations from the calculated MP2/TZVP reaction energetics of less than 5 kJ mol^{-1}. Similarly, calculations with solvent effects (toluene) had only minimal influence on the geometries and energies obtained (±5 kJ mol^{-1}). After that, this group presented variations of these calculations for beryllium and boron hydrides and for the carbene employed.[22b,c,e,g–i] This mechanism was also confirmed by work of other groups, although on different occasions the C–N bond cleavage and ring expansion of NHC was calculated to be the rate-determining step.[22d] Of interest for this work were calculations presented by Su, who evaluated the potential-energy surfaces for the ring-expansion reactions of *i*Pr_2Im with EH_2Ph_2 (E = C, Si, Ge, Sn, Pb) at the M06-2X/def2-TZVP level of theory.[22f]

These investigations suggested that the reactivity of the EH_2Ph_2 molecule that undergoes the ring-expansion reaction decreases in the order $SiH_2Ph_2 \approx GeH_2Ph_2 \approx SnH_2Ph_2 > PbH_2Ph_2 \gg CH_2Ph_2$. They also indicated that both the electronic structure and steric effects play a crucial role for the reactivity. As steric effects certainly influence the reactivity within these systems, we set out to compare the RER of the methyl-substituted NHC Me_2Im^{Me} with EH_2Ph_2 (E = Si, Ge) in some detail, and the results of the calculations performed on these systems at the M06-2x//def2-TZVPP level of theory are provided in Figure 2.

The calculations revealed for the reaction of the NHC Me_2Im^{Me} with SiH_2Ph_2 that an initial, endothermic adduct Me_2Im^{Me}·SiH_2Ph_2 **II**, five-coordinated at silicon and repulsive on the energy hyper surface by 63.0 kJ mol^{-1}, is formed. The corresponding adduct Me_2Im^{Me}·GeH_2Ph_2 lies +79.5 kJ mol^{-1} above the starting materials. The crucial transition state **TS1** for the hydrogen atom transfer can be described as an NHC–H-EHPh$_2$ σ-complex, which lies 126.4 (Si) and 134.5 kJ mol^{-1} (Ge) higher in energy compared to the starting material. This barrier agrees with the experimentally observed high temperature conditions for the RER using the silane. The Insertion product **III** lies for both, SiH_2Ph_2 and

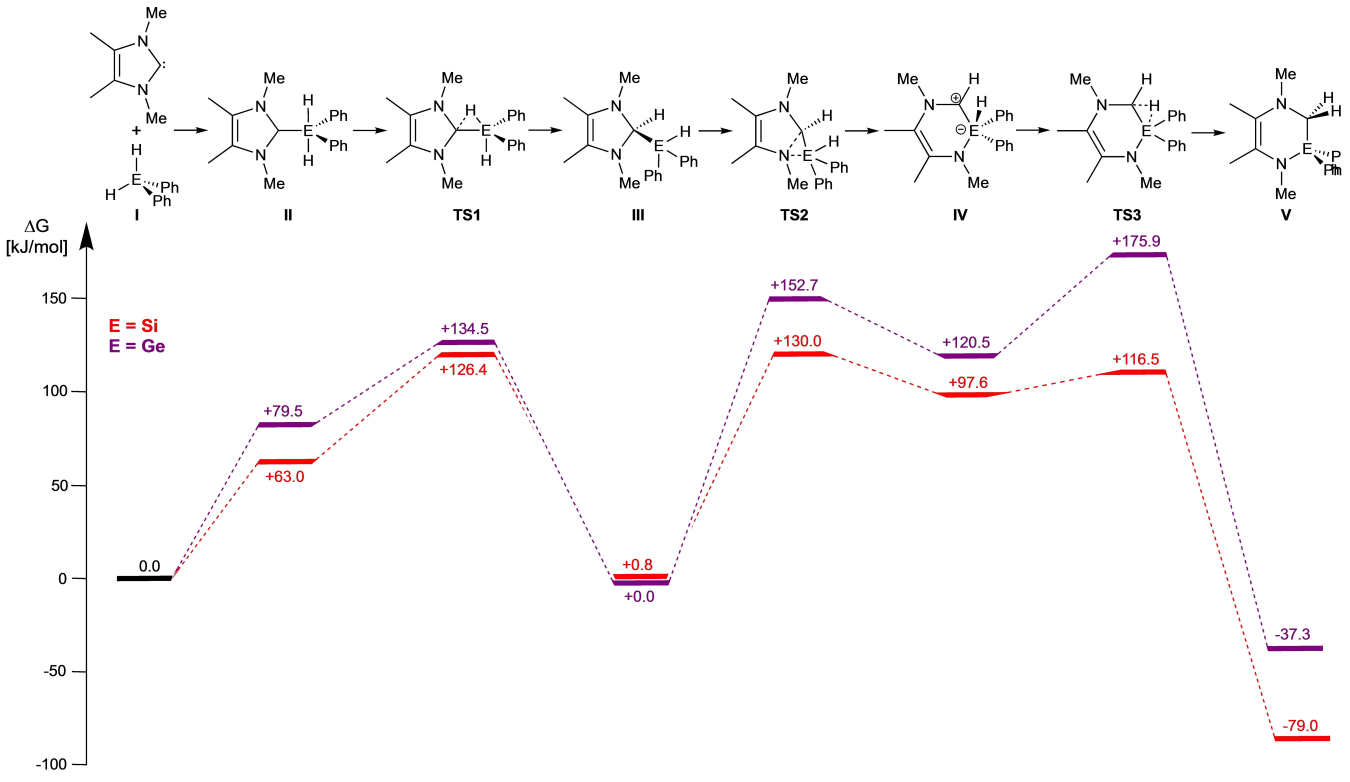

Figure 2. Molecular structures free energy profile [kJ mol^{-1}] for the RER of Me_2Im^{Me} and EH_2Ph_2 (E = Si, Ge; TURBOMOLE, M06-2x//def2-TZVPP).

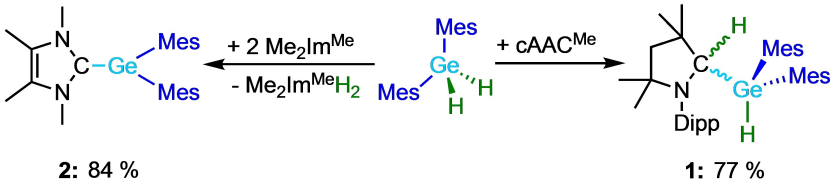

2: 84 % **1:** 77 %

Scheme 2. Reaction of $cAAC^{Me}$ and Me_2Im^{Me} with GeH_2Mes_2.

GeH_2Ph_2, within the error of the calculations at the same energy level as the starting materials. The reaction profiles for SiH_2Ph_2 and GeH_2Ph_2 then differ considerably as the pathway after the formation of adduct **III** shows significant higher barriers for the reaction of GeH_2Ph_2. The transition state **TS2** for amide transfer is calculated to be 22.7 kJ mol^{-1} higher in energy (130.0 kJ mol^{-1}, Si, vs. 152.7 kJ mol^{-1}, Ge), and the energetically very high transition state **TS3** for the hydride shift from Ge to the former NHC carbene carbon atom of 175.9 kJ mol^{-1} (instead of 116.5 kJ mol^{-1} calculated for the reaction of SiH_2Ph_2) should prevent RER for the Ge system at ambient temperatures. Therefore, another reaction pathway can be predicted, which must be evaluated experimentally.

Reaction of different carbenes with GeH_2Mes_2

We started our experimental investigations with the reaction of GeH_2Mes_2[23] and $cAAC^{Me}$ (Scheme 2). Since no reaction was observed at room temperature, the reaction mixture was heated to 85 °C overnight. Monitoring of the reaction by ^{1}H NMR spectroscopy revealed full conversion into a new compound, the cAAC insertion product into the Ge–H bond $cAAC^{Me}H$–$GeHMes_2$ (**1**, Scheme 2). A similar insertion of $cAAC^{Cy}$ into the Si–H bond of different silanes was reported previously by Bertrand and co-workers, leading to stable cAAC insertion products such as $cAAC^{Cy}H$–$SiHPh_2$.[11] Compound **1** was isolated in 77% yield by recrystallization from a saturated solution of **1** in *n*-hexane. This molecule is stable at room temperature for several weeks in solution and in the solid state.

In the ^{1}H NMR spectrum of **1** a splitting of the signal sets of the cAAC ligand was observed, which is characteristic for an asymmetric substitution at the cAAC carbene carbon atom. For instance, two doublets were detected for the CH_2 group of the $cAAC^{Me}$ at 1.72 ppm and 2.23 ppm with a coupling constant of 12.4 Hz. Additional evidence for the insertion of the carbon atom into the Ge–H bond arises from the occurrence of two doublets at 4.66 ppm and 5.95 ppm (NC*H*N and Ge*H*) with a mutual coupling constant of 6.6 Hz. In the ^{1}H,^{13}C{^{1}H} HSQC NMR spectrum of **1** the signal at 5.95 ppm does not show cross-coupling, which indicates bonding of one proton to the germanium atom. The signal at 4.66 ppm exhibits a strong coupling to the NCC(CH_3)$_2$ carbon atoms and a weak coupling to the CH_2 carbon atom, which proofs binding of the proton to the former carbene carbon atom. In addition, a band was detected at 2056 cm^{-1} in the IR spectrum of **1**, which is characteristic for a Ge–H stretching vibration and shifted hypsochromic compared to the precursor GeH_2Mes_2 ($\nu_{Ge\text{-}H}$ = 2040 cm^{-1}).[24]

Crystals of **1** suitable for X-ray diffraction were obtained from cooling an at room temperature saturated solution in *n*-hexane to −30 °C. Compound **1** crystallizes as a racemic mixture in the monoclinic space group $P2_1/c$ with one molecule in the asymmetric unit (Figure 3). The solid-state structure confirms the insertion of the cAAC into the Ge–H bond. The Ge–C1 bond length of 2.051(2) Å is unexceptional. The two hydrogen atoms located at Ge and C1 are aligned *anti* to each other in the solid state. This *anti* alignment might be forced due to the steric repulsion of the mesityl groups and the substituents of $cAAC^{Me}$.

GeH_2Mes_2 was also reacted with the NHCs Me_2Im^{Me}, iPr_2Im^{Me} and $Dipp_2Im$. No reaction occurred with the bulkier iPr_2Im^{Me} and $Dipp_2Im$, whereas heating of GeH_2Mes_2 with two equivalents Me_2Im^{Me} to 65 °C in benzene led to full conversion into Me_2Im^{Me}·$GeMes_2$ (**2**) after 10 days (Scheme 2). After the removal of all volatile material including the side product $Me_2Im^{Me}H_2$, the NHC-stabilized germylene was isolated in 84% yield. Me_2Im^{Me}·$GeMes_2$ (**2**) was synthesized before, and the NMR and IR spectroscopic data are in accordance with those reported in the literature.[25] In addition, we obtained single crystals of **2** suitable for X-ray diffraction by slow evaporation of a concentrated toluene solution of **2** at room temperature. In contrast to the orthorhombic structure reported by Baines and co-workers,[25] **2** crystallizes in our case in the monoclinic space group $P2_1/c$ (Figure 3).

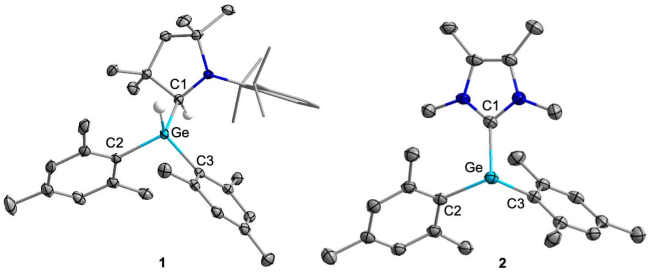

Figure 3. Molecular structures of $cAAC^{Me}H$–$GeHMes_2$ (**1**) and Me_2Im^{Me}·$GeMes_2$ (**2**), in the solid state. Hydrogen atoms and one enantiomer of the racemic mixture of **1** are omitted for clarity. Atomic displacement ellipsoids are set at 50% probability, the Dipp substituent of **1** is shown as wire-and-stick model. Selected bond lengths [Å] and angles [°]: **1**: Ge–C1, 2.026(2); Ge–C2, 1.989(2); Ge–C3, 1.997(2); C1–Ge–C2, 112.78(8); C2–Ge–C3, 107.06(8); C1–Ge–C3, 120.49(8); **2**: Ge–C1, 2.051(2); Ge–C2, 2.029(2); Ge–C3, 2.036(2); C1–Ge–C2, 103.96(9); C2–Ge–C3, 110.82(10); C1–Ge–C3, 97.63(9); N–C1–Ge–C3: 124.2(2)°.

However, there are no significant differences in the bond lengths with the reported structure, the major difference lies in the torsion angle N–C1–Ge–C3, which was reported to be 87.8(3)°)[25] and is significantly larger in our case (N–C1–Ge–C3: 124.2(2)°). Consequently the C2–Ge–C3 angle of 110.82(10)° is slightly larger compared to that reported in the literature (106.60(12)°)[25] due to lower steric repulsion of the mesityl groups with the NHC.

Reaction of carbenes with SnH_2Me_2

As the mesityl groups of GeH_2Mes_2 prevented reactions with the NHCs *i*Pr_2Im^{Me} and $Dipp_2Im$ and the Wesemann group already reported a comprehensive study on the reactivity of NHCs with aryl stannanes (see Introduction), we set out to investigate the reactivity of $cAAC^{Me}$ and the NHCs Me_2Im^{Me}, *i*Pr_2Im^{Me}, and $Dipp_2Im$ towards the steric less protected methyl-substituted stannane SnH_2Me_2. Whereas SiH_2Ph_2 and GeH_2Mes_2 react with cAACs at higher temperatures, the corresponding reaction of $cAAC^{Me}$ with SnH_2Me_2 must be performed at low temperatures to avoid side reactions (see below). The insertion product $cAAC^{Me}H–SnHMe_2$ (**3**) was obtained in 77% yield after workup (Scheme 3).

Compound **3** can be stored at −30 °C for several weeks but readily decomposes in a controlled manner in solution at room temperature to yield {$SnMe_2$} oligomeric rings (see Scheme 3 and discussion below). This reaction starts immediately after the isolated product is dissolved in solvents such as benzene, toluene or THF and typically reaches completeness at room temperature after a few days. Formation of **3** from $cAAC^{Me}$ and SnH_2Me_2 was evidenced from NMR spectroscopy. For example, the methyl groups located at tin became inequivalent in the ^{1}H NMR spectrum (Figure S6 in the Supporting Information) of **3** leading to two separate doublets, each of them equipped with ^{117}Sn and ^{119}Sn satellites, and a $^4J_{HH}$ coupling constant of 2.5 Hz. The Sn*H* resonance was detected as a doublet of septets at 5.02 ppm due to coupling to the methyl protons ($^3J_{H\text{-}H}$ = 2.5 Hz) and coupling to a single adjacent proton bound to the former carbene carbon atom ($^3J_{H\text{-}H}$ = 3.9 Hz). In addition, satellites with a $^1J_{H\text{-}^{117}Sn}$ coupling constant of 1588 Hz and a $^1J_{H\text{-}^{119}Sn}$ coupling constant of 1661 Hz were observed, which indicated direct bonding of the hydrogen atom to tin. For the proton bound to the carbenic carbon atom, a doublet with a $^3J_{H\text{-}H}$ coupling constant of 3.9 Hz was observed at 4.02 ppm with coupling constants to ^{117}Sn and ^{119}Sn of about 30.5 Hz each. The $cAAC^{Me}$ moiety gives rise to two sets of resonances due to the asymmetry of the molecule, as observed previously. In the $^{13}C\{^1H\}$ NMR spectrum a resonance at 72.0 ppm was detected for the former carbene carbon atom, which shows cross-coupling in the $^1H,^{13}C\{^1H\}$ HSQC NMR spectrum with the proton resonance at 4.02 ppm. The ^{119}Sn NMR spectrum of **3** reveals a doublet of multiplets at 139.6 ppm with a coupling constant of 1661 Hz, which collapses upon proton decoupling to a singlet. Furthermore, an IR band at 1805 cm^{-1} was assigned to the Sn–H stretching mode.[17] The solid-state structure of **3** (Figure 4) also confirms the formation of the insertion product.

Compound **3** crystallizes in the monoclinic space group $P2_1/c$ with one molecule in the asymmetric unit. The molecular structure reveals tetrahedral coordination of both the C1 carbon atom and the tin atom. The Sn–C bond lengths to the sp^3 carbon atoms are identical within 3σ (Sn–C1: 2.206(10) Å; Sn–C2: 2.163(13) Å and Sn–C3: 2.147(12) Å) and are in accordance with C–Sn single bonds. The hydrogen atoms at Sn and C1 are arranged *anti* to each other in the solid state, presumably due to steric effects, as already observed for the related germanium compound **1**.

The reaction of SnH_2Me_2 with two equivalents of Me_2Im^{Me} at room temperature led to the formation of the aminal $Me_2Im^{Me}H_2$ and the NHC-stabilized stannylene Me_2Im^{Me}·$SnMe_2$ (**4**) (Scheme 3). As the aminal $Me_2Im^{Me}H_2$ is volatile the separation is easy, and the reaction yielded **4** as a yellow solid in 67% isolated yield. Me_2Im^{Me}·$SnMe_2$ (**4**) can also be synthesized by the metallic reduction of Me_2Im^{Me}·$SnMe_2Cl_2$, which was reported, including

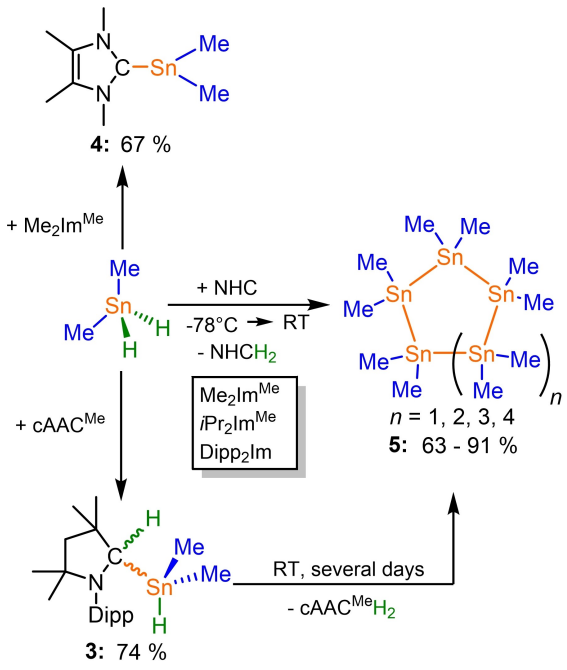

Scheme 3. Reaction of the NHCs Me_2Im^{Me}, *i*Pr_2Im^{Me}, $Dipp_2Im$ and $cAAC^{Me}$ with SnH_2Me_2.

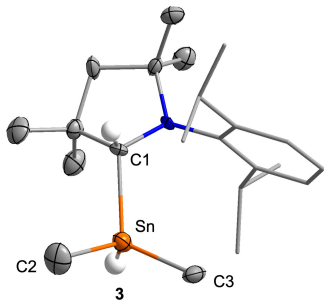

Figure 4. Molecular structure of $cAAC^{Me}H–SnHMe_2$ (**3**) in the solid state. Hydrogen atoms are omitted for clarity. Atomic displacement ellipsoids are set at 50% probability, and the Dipp substituent is shown as a wire-and-stick model. Selected bond lengths [Å] and angles [°]: Sn–C1, 2.206(10); Sn–C2, 2.163(13); Sn–C3, 2.147(12); C1–Sn–C2, 104.9(5); C2–Sn–C3, 105.4(5); C1–Sn–C3, 116.9(4).

the molecular structure of the compound (Figure S24), just recently by us.[5e]

The reaction of SnH_2Me_2 with one of the larger NHCs iPr_2Im^{Me} and $Dipp_2Im$ at low temperature did not lead to formation of NHC-stabilized stannylenes analogous to **4**. Instead, the formation of a yellow solid, sparingly soluble in toluene, and the corresponding aminal $NHCH_2$ was observed (Scheme 3). Similarly, if only one instead of two equivalents Me_2Im^{Me} was used for the synthesis of **4**, the same yellow solid was formed, which was isolated by filtration in yields of 63–91 %, depending on the NHC used. The ^{1}H NMR spectrum of this product showed only one multiplet at 0.53 ppm for equivalent methyl groups and no resonance for the NHCs used for synthesis.

The $^{119}Sn\{^1H\}$ NMR spectrum of C_6D_6 solutions of the soluble products of this reaction revealed three resonances at −246.4 ppm, −244.6 ppm, and −242.7 ppm (major component; Figure S15). A similar mixture was reported by Neumann and co-workers[26] previously, which was obtained from the equimolar condensation of SnH_2Me_2 and $SnMe_2(NEt_2)_2$. These resonances there were assigned at that time to the *cyclo*-pentamer ($\delta_{^{119}Sn} = -241.4$ ppm) and the *cyclo*-heptamer or *cyclo*-octamer ($\delta_{^{119}Sn} = -243.4$ ppm, −244.9 ppm). In addition, Neumann and co-workers observed an additional product leading to a broad and significantly more intense resonance at −231 ppm, which was assigned to the *cyclo*-hexamer. Later on, Wrackmeyer and co-workers pointed out that the intensity pattern of the ^{117}Sn satellites (2:2:1) of the signal at −241.4 ppm would correspond to the *cyclo*-hexamer.[27] Consistently, this would mean that the resonance at −231 ppm should be associated with the *cyclo*-pentamer or another oligomeric or polymeric compound.

Therefore, we assign our resonances to the *cyclo*-heptamer, the *cyclo*-octamer (−246.4 ppm, −244.6 ppm), and the *cyclo*-hexamer (−242.7 ppm) as the main products of the solution. Even with high resolution $^{119}Sn\{^1H\}$ NMR experiments we were not able to resolve different resonances or use coupling constants to clarify the assignment of the *cyclo*-heptamer and the *cyclo*-octamer to the corresponding signals.

As the tin *cyclo*-oligomers were reported to be well soluble substances in various hydrocarbons,[26] we further investigated the poorly soluble yellow solid by using solid-state NMR spectroscopy (Figures S14–S16). In both the ^{1}H DP/MAS and $^{13}C\{^1H\}$ CP/MAS solid state NMR spectra a singlet was detected at 0.92 and −10.4 ppm, respectively, for the methyl groups (Figures S16 and S17). In contrast to the $^{119}Sn\{^1H\}$ NMR investigations in solution, only one signal was detected at −226.0 ppm in the $^{119}Sn\{^1H\}$ CP/MAS solid state NMR spectrum (Figure S18). As the NMR shifts obtained from solution NMR and solid-state NMR are often difficult to compare, the only conclusion that can be made is that the yellow solid contains only one product of (nearly) equivalent tin atoms. Interestingly, the yellow solid dissolves completely after heating in benzene to 80 °C for a few seconds. In addition to the resonances obtained for the solution of the product, as discussed above, new broad resonances were detected in the ^{1}H and $^{119}Sn\{^1H\}$ NMR spectra of the resulting solution at 0.64 ppm (^{1}H NMR) and −232.4 ppm ($^{119}Sn\{^1H\}$ NMR), respectively (Figures S19 and S20). We attribute the latter to the *cyclo*-pentamer and assume that the ^{119}Sn solid-state NMR resonance at −226.0 ppm is the signal of the *cyclo*-pentamer. Note that the resonances typically observed for chain oligomers or polymers, that is, alkyl-substituted polystannanes, are typically observed in the range between −172.2 ppm to −194.8 ppm in their solution ^{119}Sn NMR spectra.[28] Thus, the *cyclo*-pentamer *cyclo*-$(SnMe_2)_5$ seems to be the favored product of the DHC of SnH_2Me_2 with the NHCs Me_2Im^{Me}, iPr_2Im^{Me}, and $Dipp_2Im$ (isolation in 63–91 % yield). Unfortunately, we could not obtain crystals of this product suitable for X-ray diffraction or meaningful high-resolution mass-spectrometry data of this product.

Interestingly, a mixture of *cyclo*-stannanes can also be obtained from the decomposition of $cAAC^{Me}H–SnHMe_2$ (**3**). We noted before that **3** easily decomposes in a controlled manner, and the reaction products of this decomposition are *cyclo*-stannanes (Figures S21–S23) and $cAAC^{Me}H_2$, which can be easily detected in the ^{1}H NMR spectrum. However, for the DHC using $cAAC^{Me}H–SnHMe_2$ (**3**) only the *cyclo*-heptamer, the *cyclo*-octamer (−246.4 ppm, −244.6 ppm), and the *cyclo*-hexamer (−242.7 ppm) were formed.

As oligomer mixtures were obtained from the DHC of SnH_2Me_2 using one equivalent of the NHC Me_2Im^{Me}, iPr_2Im^{Me} and $Dipp_2Im$ at room temperature or by heating a benzene solution of compound **3** to 80 °C overnight, we assume that insertion products of the carbene into the Sn–H bond and reductive elimination of $NHCH_2$ and/or $cAACH_2$ play a major role in the formation of these tin *cyclo*-oligomers of different sizes.

Conclusion

This work is based on our previous studies on the reactivity of silicon element hydrides SiH_3Ph, SiH_2Ph_2 and $SiHPh_3$ with different NHCs, which led to the formation of diaza-silinanes with insertion of silylene moieties into the C–N bond of the NHCs and thus to a ring expansion reaction (RER) of the NHC. DFT calculations on the RER of Me_2Im^{Me} with EH_2Ph_2 (E = Si, Ge) predicted different reaction pathways for the corresponding germane. Therefore, the reactivity of several different NHCs and the cyclic (alkyl)(amino)carbene $cAAC^{Me}$ with the group 14 hydrides GeH_2Mes_2 and SnH_2Me_2 was investigated.

The reaction of GeH_2Mes_2 with $cAAC^{Me}$ led to insertion of the cAAC carbene carbon atom into one of the Ge–H bonds and formation of $cAAC^{Me}H–GeHMes_2$ (**1**). Similar products of the insertion $cAAC^{Cy}$ into the Si–H bond of silanes were reported previously by Bertrand and co-workers. The reaction of GeH_2Mes_2 with two equivalents of Me_2Im^{Me} at elevated temperatures led to dehydrogenation of GeH_2Mes_2. One equivalent of the NHC acts as excellent hydrogen acceptor and yields $NHCH_2$, the other equivalent NHC stabilizes the resulting germylene $GeMes_2$ to yield $Me_2Im^{Me}\cdot GeMes_2$ (**2**). In analogy, the reaction of SnH_2Me_2 with $cAAC^{Me}$ afforded the insertion product $cAAC^{Me}H–SnHMe_2$ (**3**). Dehydrogenation of SnH_2Me_2 by using Me_2Im^{Me} also led to the formation of a NHC-stabilized stannylene, that is, $Me_2Im^{Me}\cdot SnMe_2$ (**4**). The use of just one equivalent Me_2Im^{Me} or of the sterically more demanding NHCs iPr_2Im^{Me} and $Dipp_2Im$ afforded tin *cyclo*-oligomers $(SnMe_2)_n$ (**5**;

n = 6–8), products of a coupling reaction of the {$SnMe_2$} moieties formed in situ by dehydrogenation . The pentamer *cyclo*-$(SnMe_2)_5$ seems to be the dominant product of this reaction, and the compound was isolated in 63 to 91 % yield. A mixture of cyclostannanes was also obtained from the decomposition of cAAC^{Me}H–$SnHMe_2$ (**3**) with formation of cAAC$^{Me}H_2$. We were not successful in obtaining oligomer mixtures from the isolated NHC-stabilized stannylene Me_2Im^{Me}·$SnMe_2$ (**4**); this contrasts with the situation observed for phosphines.[12] The dehydrogenative coupling of primary and secondary phosphines with NHCs afforded diphosphines R_2P–PR_2 for secondary phosphines and mixtures of NHC phosphinidene adducts NHC=PAr and cyclic oligophosphines P_4Ar_4, P_5Ar_5 and P_6Ar_6, depending on the stoichiometry used. NHC phosphinidene adducts can act as synthons for phosphinidene moieties [PAr], which oligomerize in an equilibrium to give the *cyclo*-oligophosphines. As this reactivity was not observed for the NHC stannylene **4**, we currently assume that insertion products of the carbene into the Sn–H bond and reductive elimination of $NHCH_2$ and/or $cAACH_2$ with liberation of $SnMe_2$ and subsequent oligomerization or more complex reaction mechanisms play a major role in the formation of the tin *cyclo*-oligomers of different sizes.

Experimental Section

General considerations, instrumentation, and synthesis of starting material are provided in the Supporting Information. ^{1}H and $^{13}C\{^1H\}$ NMR chemical shifts are listed in parts per million (ppm).

Synthesis and characterization of the compounds

cAAC^{Me}H<C->GeHMes$_2$ (1): A solution of GeH_2Mes_2 (110 mg, 351 μmol, 1.0 equiv.) and cAAC^{Me} (100 mg, 351 μmol, 1.0 equiv.) in toluene (10 mL) was stirred at 85 °C overnight. After removing all volatiles in vacuo, *n*-hexane (10 mL) was added to the remaining solid. The resulting suspension was filtered, and the filtrate subsequently concentrated to a volume of 5 mL. Storing the concentrate at −30 °C for 2 weeks yielded **1** (162 mg, 468 μmol, 77 %) as a colorless solid. Crystals suitable for single-crystal X-ray diffraction were obtained by slow evaporation of a concentrated toluene solution of **1** at room temperature. Elemental analysis (%) calcd. for $C_{38}H_{55}GeN$ [598.50 g mol^{-1}]: C 76.26, H 9.26, N 2.34; found: C 76.52, H 9.26, N 2.43. IR ([cm^{-1}]): 3019 (vw), 3001 (w), 2991 (w), 2967 (m), 2938 (m), 2910 (m), 2869 (w), 2056 (Ge–H, m), 1601 (w), 1552 (vw), 1468 (m), 1449 (m), 1436 (s), 1410 (w), 1366 (m), 1313 (m), 1248 (w), 1194 (m), 1175 (w), 1165 (w), 1123 (w), 1096 (vw), 1064 (m), 1048 (w), 1030 (w), 1014 (w), 958 (vw), 926 (w), 907 (vw), 888 (vw), 850 (m), 842 (m), 806 (vs), 769 (vs), 704 (m), 672 (vw), 635 (vw), 600 (w), 583 (m), 566 (w), 550 (m), 539 (m), 496 (vw), 476 (vw), 444 (w), 420 (vw). ^{1}H NMR (500.1 MHz, C_6D_6, 298 K): δ = 0.60 (d, 3 H, $^3J_{H\text{-}H}$ = 6.9 Hz, *i*Pr-CH_3), 0.92 (s, 3 H, NC(CH_3)$_2$), 1.14 (d, 3 H, $^3J_{H\text{-}H}$ = 6.9 Hz, *i*Pr-CH_3), 1.27 (d, 3 H, $^3J_{H\text{-}H}$ = 6.9 Hz, *i*Pr-CH_3), 1.28 (s, 3 H, NC(CH_3)$_2$), 1.43 (d, 3 H, $^3J_{H\text{-}H}$ = 6.9 Hz, *i*Pr-CH_3), 1.56 (s, 3 H, NCC(CH_3)$_2$), 1.71 (s, 3 H, NCC(CH_3)$_2$), 1.72 (d, 1 H, $^2J_{H\text{-}H}$ = 12.4 Hz, CH_2), 1.74 (br, 3 H, Mes-*o*-CH_3), 1.97 (s, 3 H, Mes-*p*-CH_3), 2.07 (s, 3 H, Mes-*p*-CH_3), 2.23 (d, 1 H, $^2J_{H\text{-}H}$ = 12.4 Hz, CH_2), 2.36 (br, 3 H, Mes-*o*-CH_3), 2.46 (br, 3 H, Mes-*o*-CH_3), 2.83 (br, 3 H, Mes-*o*-CH_3), 3.39 (sept, 2 H, $^3J_{H\text{-}H}$ = 6.9 Hz, *i*Pr-C*H*), 4.08 (sept, 2 H, $^3J_{H\text{-}H}$ = 6.9 Hz, *i*Pr-C*H*), 4.66 (d, 1 H, $^3J_{H\text{-}H}$ = 6.6 Hz, NC*H*N), 5.95 (d, 1 H, $^3J_{H\text{-}H}$ = 6.6 Hz, Ge*H*), 6.57 (br, 3 H, Mes-C*H* overlapped by Mes-C*H*), 6.87 (br, 1 H, Mes-C*H*), 6.95 (dd, 1 H, $^3J_{H\text{-}H}$ = 7.6 Hz, $^4J_{H\text{-}H}$ = 1.9 Hz, Dipp-*m*-C*H*), 7.09 (dd, 1 H, $^3J_{H\text{-}H}$ = 7.6 Hz, $^4J_{H\text{-}H}$ = 1.9 Hz, Dipp-*m*-C*H*), 7.15 (t, 2 H, $^3J_{H\text{-}H}$ = 7.6 Hz, Dipp-*p*-C*H*). $^{13}C\{^1H\}$ NMR (125.8 MHz, C_6D_6, 298 K): δ = 20.8 (Mes-*p*-CH_3), 21.0 (Mes-*p*-CH_3), 22.6 (*i*Pr-CH_3), 23.5 (Mes-*o*-CH_3), 24.2 (Mes-*o*-CH_3), 24.8 (*i*Pr-CH_3), 24.9 (Mes-*o*-CH_3), 25.3 (Mes-*o*-CH_3), 25.5 (*i*Pr-CH_3), 27.5 (*i*Pr-CH_3), 27.9 (*i*Pr-CH), 28.07 (NC(CH_3)$_2$), 28.09 (*i*Pr-CH), 29.7 (NCC(CH_3)$_2$), 32.2 (NCC(CH_3)$_2$), 33.1 (NC(CH_3)$_2$), 44.3 (NC(CH_3)$_2$), 60.5 (CH_2), 64.2 (NCC(CH_3)$_2$), 75.0 (NCGe), 124.6 (Dipp-*m*-CH), 125.4 (Dipp-*m*-CH), 127.1 (Dipp-*p*-CH), 128.8 (Mes-*m*-CH), 129.5 (Mes-*m*-CH), 135.6 (Mes-*i*-C), 137.6 (Mes-*p*-C), 137.7 (Mes-*p*-C), 140.7 (Mes-*i*-C), 142.0 (Mes-*o*-C), 142.8 (Mes-*o*-C), 143.8 (Mes-*p*-C), 143.9 (Mes-*o*-C), 144.4 (Mes-*o*-C), 149.5 (Dipp-*o*-C), 152.4 (Dipp-*o*-C).

Me_2Im^{Me}·GeMes$_2$ (2): A solution of GeH_2Mes_2 (126 mg, 403 μmol, 1.0 equiv.) in benzene (5 mL) was added to a solution of Me_2Im^{Me} (100 mg, 805 μmol, 2.0 equiv.) in benzene (5 mL) and the resulting mixture was heated for 10 d to 65 °C under stirring. All volatiles (including the side product $Me_2Im^{Me}H_2$) were removed in vacuo to yield **2** (148 mg, 340 μmol, 84 %) as a colorless solid. Crystals suitable for single-crystal X-ray diffraction were obtained by slow evaporation of a concentrated toluene solution of **2** at room temperature. Elemental analysis (%) calcd. for $C_{25}H_{34}GeN_2$ (435.19 g mol^{-1}): C 69.00, H 7.88, N 6.44; found: C 66.38, H 7.73, N 5.89. After several attempts, this is the best result so far, which may be due to the high sensitivity of **2**. ^{1}H NMR (500.1 MHz, C_6D_6, 298 K): δ = 1.13 (s, 6 H, NCCH_3), 2.30 (s, 6 H, Mes-*p*-CH_3), 2.63 (s, 6 H, Mes-*o*-CH_3), 3.05 (s, 6 H, NCH_3), 6.97 (4 H, Mes-*m*-C*H*). $^{13}C\{^1H\}$ NMR (125.8 MHz, C_6D_6, 298 K): δ = 8.0 (CCH_3), 21.3 (Mes-*p*-CH_3), 25.6 (Mes-*o*-CH_3), 32.9 (NCH_3), 124.8 (NCCH_3), 128.6 (Mes-*m*-CH), 134.8 (Mes-*p*-C), 144.5 (Mes-*o*-C), 151.3 (Mes-*i*-C), 175.4 (NCN).

cAAC^{Me}H<C->SnHMe$_2$ (3): A solution of SnH_2Me_2 (288 mg, 1.91 mmol, 1.0 equiv.) in *n*-hexane (5 mL) was added to a solution of cAAC^{Me} (546 mg, 351 μmol, 1.0 equiv.) in *n*-hexane (5 mL) at −78 °C and allowed to warm over a period of 2 h. Removing all volatiles in vacuo yielded **3** (162 mg, 468 μmol, 77 %) as a colorless solid. Crystals suitable for single-crystal X-ray diffraction were obtained by slow evaporation of a concentrated toluene solution of **3** at room temperature. Elemental analysis (%) calcd. for $C_{22}H_{39}NSn$ (436.27 g mol^{-1}): C 60.57, H 9.01, N 3.21; found: C 60.94, H 9.41, N 3.17. IR ([cm^{-1}]): 3051 (vw), 2962 (m), 2938 (m), 2935 (m), 2866 (m), 2754 (w), 1805 (Sn–H, s), 1573 (vw), 1458 (m), 1436 (m), 1383 (m), 1364 (m), 1324 (w), 1310 (w), 1288 (w), 1257 (w), 1249 (w), 1210 (m), 1173 (vw), 1156 (m), 1105 (w), 1070 (vw), 1045 (w), 1012 (vw), 953 (vw), 927 (vw), 884 (vw), 810 (m), 772 (s), 707 (w), 685 (w), 654 (m), 607 (vw), 595 (vw), 573 (m), 557 (w), 509 (vs), 468 (w), 437 (w), 407 (vw). ^{1}H NMR (500.1 MHz, C_6D_6, 298 K): δ = −0.28 (d, 3 H, $^3J_{H\text{-}H}$ = 2.6 Hz, $^2J_{H\text{-}^{117}Sn}$ = 52.2 Hz, $^2J_{H\text{-}^{119}Sn}$ = 54.2 Hz, Sn-CH_3), 0.07 (d, 3 H, $^3J_{H\text{-}H}$ = 2.6 Hz, $^2J_{H\text{-}^{117}Sn}$ = 49.5 Hz, $^2J_{H\text{-}^{117}Sn}$ = 51.5 Hz, Sn-CH_3), 1.07 (s, 3 H, NCC(CH_3)$_2$), 1.11 (s, 3 H, NCC(CH_3)$_2$), 1.21 (d, 3 H, $^3J_{H\text{-}H}$ = 6.7 Hz, *i*Pr-CH_3), 1.22 (d, 3 H, $^3J_{H\text{-}H}$ = 6.7 Hz, *i*Pr-CH_3), 1.27 (d, 6 H, $^3J_{H\text{-}H}$ = 6.7 Hz, *i*Pr-CH_3), 1.33 (s, 3 H, NC(CH_3)$_2$), 1.48 (s, 3 H, NC(CH_3)$_2$), 1.78 (d, 1 H, $^2J_{H\text{-}H}$ = 12.5 Hz, CH_2), 1.82 (d, 1 H, $^2J_{H\text{-}H}$ = 12.5 Hz, CH_2), 3.38 (sept, 1 H, $^3J_{H\text{-}H}$ = 6.9 Hz, *i*Pr-C*H*), 4.00 (sept, 1 H, $^3J_{H\text{-}H}$ = 6.9 Hz, *i*Pr-C*H*), 4.02 (d, 1 H, $^3J_{H\text{-}H}$ = 3.9 Hz, overlapping satellites: $^2J_{H\text{-}^{117}Sn}$ = 30.5 Hz, $^2J_{H\text{-}^{119}Sn}$ = 30.5 Hz, NC*H*N), 5.02 (dsept, 1 H, $^3J_{H\text{-}H}$ = 2.6 Hz, $^3J_{H\text{-}H_{(NCHN)}}$ = 3.9 Hz, $^1J_{H\text{-}^{117}Sn}$ = 1588 Hz, $^1J_{H\text{-}^{119}Sn}$ = 1661 Hz, Sn*H*), 7.06 (t, 1 H, $^3J_{H\text{-}H}$ = 4.7 Hz, Dipp-*p*-C*H*), 7.14 (d, 2 H, $^3J_{H\text{-}H}$ = 4.7 Hz, Dipp-*m*-C*H*). $^{13}C\{^1H\}$ NMR (125.8 MHz, C_6D_6, 298 K): δ = −10.6 (SnCH_3), −10.3 (SnCH_3), 24.7 (*i*Pr-CH_3), 25.7 (*i*Pr-CH_3), 25.9 (*i*Pr-CH_3), 26.0 (*i*Pr-CH_3), 27.1 (*i*Pr-CH), 29.2 (NCC(CH_3)$_2$), 29.4 (NCC(CH_3)$_2$), 29.6 (*i*Pr-CH), 30.6 (NC(CH_3)$_2$), 31.9 (NC(CH_3)$_2$), 41.1 (NCC(CH_3)$_2$), 58.6 (CH_2), 63.9 (NC(CH_3)$_2$), 72.0 (NCHN), 125.1 (Dipp-*m*-CH), 125.6 (Dipp-*p*-CH), 127.2 (Dipp-*m*-CH), 140.9 (Dipp-*i*-CH), 151.4 (Dipp-*o*-C), 151.5 (Dipp-*o*-C). $^{119}Sn\{^1H\}$ NMR (186.5 MHz, C_6D_6, 298 K): δ = −139.6 (s). ^{119}Sn NMR (186.5 MHz, C_6D_6, 298 K): δ = −139.6 (dm, $^1J_{H\text{-}^{119}Sn}$ = 1661 Hz).

$Me_2Im^{Me}\cdot SnMe_2$ (4): A solution of SnH_2Me_2 (282 mg, 1.87 mmol, 1.0 equiv.) in toluene (5 mL) was added to a solution of Me_2Im^{Me} (465 mg, 3.74 mmol, 2.0 equiv.) in toluene (5 mL) at −78 °C and the resulting mixture was allowed to warm to room temperature over a period of 2 h. All volatiles (including the side product $Me_2Im^{Me}H_2$) were removed in vacuo to yield **4** (340 mg, 1.25, mmol, 67 %) as a yellow solid. Crystals suitable for single-crystal X-ray diffraction were obtained by slow evaporation of a concentrated toluene solution of **4** at room temperature. Elemental analysis (%) calcd. for $C_9H_{18}SnN_2$ (272.97 g mol^{-1}): C 39.60, H 6.65, N 10.26; found: C 36.93, H 6.40, N 8.91. After several attempts, this is the best result so far, which may be due to the high air sensitivity of **4**. IR ([cm^{-1}]): 2977 (w), 2947 (m), 2919 (m), 1897 (m), 1855 (w), 1784 (vw), 1688 (w), 1662 (m), 1649 (m), 1598 (w), 1574 (w), 1455 (m), 1431 (s), 1396 (m), 1374 (s), 1366 (s), 1309 (w), 1226 (w), 1194 (w), 1122 (vw), 1095 (vw), 965 (m), 844 (m), 754 (s), 732 (s), 712 (m), 664 (w), 569 (s), 549 (s), 515 (w), 475 (vw), 449 (vs). ^{1}H NMR (500.1 MHz, C_6D_6, 298 K): $\delta =$ 0.73 (s, 6 H, overlapping broad satellites, SnCH_3), 1.31 (s, 6 H, NCCH_3), 3.19 (s, 6 H, NCH_3). ^{13}C{^{1}H} NMR (125.8 MHz, C_6D_6, 298 K): $\delta =$ 0.5 (SnCH_3), 8.3 (CCH_3), 34.4 (NCH_3), 124.2 (NCCH_3), 183.4 (NCN). ^{119}Sn{^{1}H} NMR (186.5 MHz, C_6D_6, 298 K): $\delta = -83.3$.

$(SnMe_2)_n$ (5): *Route A*: A solution of SnH_2Me_2 (317 mg, 2.10 mmol, 1.0 equiv.) in toluene (10 mL) was added to a solution of $Dipp_2Im$ (817 mg, 2.10 mmol, 1.0 equiv.) in toluene (10 mL) at −78 °C, and the resulting mixture was allowed to warm to room temperature overnight. All volatiles were removed in vacuo to obtain a yellow solid. The crude product was washed with *n*-hexane (3 x 12 mL) to remove the $Dipp_2ImH_2$ yielding **5** (120 mg, 223 μmol, 63 %) as a yellow solid. *Route B*: A solution of SnH_2Me_2 (313 mg, 2.08 mmol, 1.0 equiv.) in toluene (10 mL) was added to a solution of Me_2Im^{Me} (206 mg, 1.66 mmol, 0.8 equiv.) in toluene (10 mL) at −78 °C, and the resulting mixture was allowed to warm to room temperature overnight. All volatiles (including the side product $Me_2Im^{Me}H_2$ and excess SnH_2Me_2) were removed in vacuo to yield **5** (224 mg, 1.51 mmol, 91 %) as a yellow solid. Elemental analysis (%) calcd. for *n* x C_2H_6Sn [*n* x 148.78 g mol^{-1}]: C 16.15, H 4.07; found: C 18.75, H 4.12. After several attempts, this is the best result, which may be due to the high sensitivity of **5**. IR ([cm^{-1}]): 2966 (w), 2905 (m), 2330 (w), 1670 (vw), 1532 (vw), 1457 (w), 1385 (vw), 1367 (vw), 1328 (vw), 1254 (vw), 1204 (vw), 1182 (m), 1056 (m), 1034 (m), 953 (vw), 936 (vw), 768 (s), 702 (vs), 510 (vs), 493 (vs). ^{1}H NMR (500.1 MHz, C_6D_6, 298 K): $\delta =$ 0.53 (m). ^{13}C{^{1}H} NMR (125.8 MHz, C_6D_6, 298 K): $\delta =$ −12.3. ^{119}Sn{^{1}H} NMR (186.5 MHz, C_6D_6, 298 K): $\delta = -246.4$ ($(SnMe_2)_{7/8}$), −244.6 ($(SnMe_2)_{7/8}$), −242.7 ($(SnMe_2)_6$). ^{1}H DP/MAS NMR solid state (400.1 MHz, 295 K, $\nu_{Mas} = 14.8$ kHz): $\delta = 0.92$ (s_{br}). ^{13}C{^{1}H} CP/MAS NMR solid state (100.6 MHz, 295 K, $\nu_{Mas} = 13.5$ kHz, contact time: 2.00 ms): $\delta = -10.4$ (s). ^{119}Sn{^{1}H} CP/MAS NMR solid state (149.2 MHz, 295 K, $\nu_{Mas} = 14.8$ kHz, contact time: 5.00 ms): $\delta =$ −226.0 (CSA: $\delta_{11} = -110.35$, $\delta_{22} = -233.27$, $\delta_{33} = -337.02$). NMR spectra after heating the mixture of the cyclomers: ^{1}H NMR (500.1 MHz, C_6D_6, 298 K): $\delta = 0.53$ (m) 0.64 (m). ^{119}Sn{^{1}H} NMR (186.5 MHz, C_6D_6, 298 K): $\delta = -246.4$ ($(SnMe_2)_{7/8}$), −244.6 ($(SnMe_2)_{7/8}$), −242.7 ($(SnMe_2)_6$), −232.4.

Computational details: Computational details are provided in the Supporting Information.

Crystallographic details: Crystal data collection and processing parameters are given in the Supporting Information. Deposition Numbers 2195878 (**3**), 2195879 (**1**), 2195880 (**2**) contain the supplementary crystallographic data for this paper. These data are provided free of charge by the joint Cambridge Crystallographic Data Centre and Fachinformationszentrum Karlsruhe Access Structures service.

Acknowledgements

This work was supported by the Julius-Maximilians-Universität Würzburg and the Deutsche Forschungsgemeinschaft (DFG; RA720/13+project no. 466754611). Open Access funding enabled and organized by Projekt DEAL.

Conflict of Interest

The authors declare no conflict of interest.

Data Availability Statement

The data that support the findings of this study are available in the supplementary material of this article.

Keywords: cyclic alkyl(amino)carbenes · germanium · hydrides · N-heterocyclic carbenes · tin

[1] a) W. A. Herrmann, C. Köcher, *Angew. Chem. Int. Ed.* **1997**, *36*, 2162–2187; *Angew. Chem.* **1997**, *109*, 2256–2282; b) P. P. Power, *Chem. Rev.* **1999**, *99*, 3463–3504; c) D. Bourissou, O. Guerret, F. P. Gabbai, G. Bertrand, *Chem. Rev.* **2000**, *100*, 39–92; d) F. E. Hahn, M. C. Jahnke, *Angew. Chem. Int. Ed.* **2008**, *47*, 3122–3172; *Angew. Chem.* **2008**, *120*, 3166–3216; e) T. Dröge, F. Glorius, *Angew. Chem. Int. Ed.* **2010**, *49*, 6940–6952; *Angew. Chem.* **2010**, *122*, 7094–7107; f) Y. Wang, G. H. Robinson, *Inorg. Chem.* **2011**, *50*, 12326–12337; g) M. N. Hopkinson, C. Richter, M. Schedler, F. Glorius, *Nat. Chem.* **2014**, *510*, 485–496; h) Y. Wang, G. H. Robinson, *Inorg. Chem.* **2014**, *53*, 11815–11832; i) S. Würtemberger-Pietsch, U. Radius, T. B. Marder, *Dalton Trans.* **2016**, *45*, 5880–5895; j) V. Nesterov, D. Reiter, P. Bag, P. Frisch, R. Holzner, A. Porzelt, S. Inoue, *Chem. Rev.* **2018**, *118*, 9678–9842; k) A. Doddi, M. Peters, M. Tamm, *Chem. Rev.* **2019**, *119*, 6994–7112.

[2] a) M. Melaimi, M. Soleilhavoup, G. Bertrand, *Angew. Chem. Int. Ed.* **2010**, *49*, 8810–8849; *Angew. Chem.* **2010**, *122*, 8992–9032; b) M. Soleilhavoup, G. Bertrand, *Acc. Chem. Res.* **2015**, *48*, 256–266; c) M. Melaimi, R. Jazzar, M. Soleilhavoup, G. Bertrand, *Angew. Chem. Int. Ed.* **2017**, *56*, 10046–10068; *Angew. Chem.* **2017**, *129*, 10180–10203; d) U. S. Paul, U. Radius, *Chem. Eur. J.* **2017**, *23*, 3993–4009; e) U. S. D. Paul, M. J. Krahfuß, U. Radius, *Chem. Unserer Zeit* **2019**, *53*, 212–223.

[3] a) R. Dorta, E. D. Stevens, N. M. Scott, C. Costabile, L. Cavallo, C. D. Hoff, S. P. Nolan, *J. Am. Chem. Soc.* **2005**, *127*, 2485–2495; b) S. Diez-Gonzalez, S. P. Nolan, *Coord. Chem. Rev.* **2007**, *251*, 874–883; c) A. Poater, B. Cosenza, A. Correa, S. Giudice, F. Ragone, V. Scarano, L. Cavallo, *Eur. J. Inorg. Chem.* **2009**, 1759–1766; d) H. Clavier, S. P. Nolan, *Chem. Commun.* **2010**, *46*, 841–861; e) C. Lujan, S. P. Nolan, *J. Organomet. Chem.* **2011**, *696*, 3935–3938; f) O. Back, M. Henry-Ellinger, C. D. Martin, D. Martin, G. Bertrand, *Angew. Chem. Int. Ed.* **2013**, *52*, 2939–2943; *Angew. Chem.* **2013**, *125*, 3011–3015; g) A. Liske, K. Verlinden, H. Buhl, K. Schaper, C. Ganter, *Organometallics* **2013**, *32*, 5269–5272; h) D. J. Nelson, S. P. Nolan, *Chem. Soc. Rev.* **2013**, *42*, 6723–6753; i) K. Verlinden, H. Buhl, W. Frank, C. Ganter, *Eur. J. Inorg. Chem.* **2015**, 2416–2425; j) S. V. C. Vummaleti, D. J. Nelson, A. Poater, A. Gomez-Suarez, D. B. Cordes, A. M. Z. Slawin, S. P. Nolan, L. Cavallo, *Chem. Sci.* **2015**, *6*, 1895–1904; k) K. C. Mondal, S. Roy, B. Maity, D. Koley, H. W. Roesky, *Inorg. Chem.* **2016**, *55*, 163–169; l) U. S. D. Paul, U. Radius, *Eur. J. Inorg. Chem.* **2017**, 3362–3375; m) H. V. Huynh, *Chem. Rev.* **2018**, *118*, 9457–9492; n) D. Munz, *Organometallics* **2018**, *37*, 275–289.

[4] a) S. Pietsch, U. Paul, I. A. Cade, M. J. Ingleson, U. Radius, T. B. Marder, *Chem. Eur. J.* **2015**, *21*, 9018–9021; b) S. Würtemberger-Pietsch, H. Schneider, T. B. Marder, U. Radius, *Chem. Eur. J.* **2016**, *22*, 13032–13036; c) M. Eck, S. Würtemberger-Pietsch, A. Eichhorn, J. H. Berthel, R. Bertermann, U. S. Paul, H. Schneider, A. Friedrich, C. Kleeberg, U. Radius, T. B. Marder, *Dalton Trans.* **2017**, *46*, 3661–3680; d) A. F. Eichhorn, S. Fuchs, M. Flock, T. B. Marder, U. Radius, *Angew. Chem. Int. Ed.* **2017**, *56*,

10209–10213; *Angew. Chem.* **2017**, *129*, 10343–10347; e) A. F. Eichhorn, L. Kuehn, T. B. Marder, U. Radius, *Chem. Commun.* **2017**, *53*, 11694–11696; f) H. Schneider, A. Hock, R. Bertermann, U. Radius, *Chem. Eur. J.* **2017**, *23*, 12387–12398; g) A. Hock, H. Schneider, M. J. Krahfuss, U. Radius, *Z. Anorg. Allg. Chem.* **2018**, *644*, 1243–1251; h) H. Schneider, A. Hock, A. D. Jaeger, D. Lentz, U. Radius, *Eur. J. Inorg. Chem.* **2018**, 4031–4043; i) L. Kuehn, M. Stang, S. Würtemberger-Pietsch, A. Friedrich, H. Schneider, U. Radius, T. B. Marder, *Faraday Discuss.* **2019**, *220*, 350–363; j) A. Hock, L. Werner, C. Luz, U. Radius, *Dalton Trans.* **2020**, *49*, 11108–11119; k) A. Hock, L. Werner, M. Riethmann, U. Radius, *Eur. J. Inorg. Chem.* **2020**, 4015–4023; l) S. A. Föhrenbacher, V. Zeh, M. Krahfuss, N. V. Ignat'ev, M. Finze, U. Radius, *Eur. J. Inorg. Chem.* **2021**, 1941–1960; m) M. S. M. Philipp, M. J. Krahfuss, K. Radacki, U. Radius, *Eur. J. Inorg. Chem.* **2021**, 4007–4019; n) M. S. M. Philipp, U. Radius, *Z. Anorg. Allg. Chem.* **2022**, e202200085.

[5] a) D. Schmidt, J. H. J. Berthel, S. Pietsch, U. Radius, *Angew. Chem. Int. Ed.* **2012**, *51*, 8881–8885; *Angew. Chem.* **2012**, *124*, 9011–9015; b) P. Hemberger, A. Bodi, J. H. Berthel, U. Radius, *Chem. Eur. J.* **2015**, *21*, 1434–1438; c) H. Schneider, D. Schmidt, U. Radius, *Chem. Eur. J.* **2015**, *21*, 2793–2797; d) H. Schneider, M. J. Krahfuß, U. Radius, *Z. Anorg. Allg. Chem.* **2016**, *642*, 1282–1286; e) M. S. M. Philipp, R. Bertermann, U. Radius, *Eur. J. Inorg. Chem.* **2022**, e202200429.

[6] a) M. Eck, S. Würtemberger-Pietsch, A. Eichhorn, J. H. Berthel, R. Bertermann, U. S. Paul, H. Schneider, A. Friedrich, C. Kleeberg, U. Radius, T. B. Marder, *Dalton Trans.* **2017**, *46*, 3661–3680; b) J. Lorkowski, M. Krahfuss, M. Kubicki, U. Radius, C. Pietraszuk, *Chem. Eur. J.* **2019**, *25*, 11365–11374.

[7] a) M. Arrowsmith, M. S. Hill, G. Kociok-Köhn, D. J. MacDougall, M. F. Mahon, *Angew. Chem. Int. Ed.* **2012**, *51*, 2098–2100; *Angew. Chem.* **2012**, *124*, 2140–2142; b) M. Arrowsmith, M. S. Hill, G. Kociok-Köhn, *Organometallics* **2015**, *34*, 653–662.

[8] a) S. M. Al-Rafia, R. McDonald, M. J. Ferguson, E. Rivard, *Chem. Eur. J.* **2012**, *18*, 13810–13820; b) S. K. Bose, K. Fucke, L. Liu, P. G. Steel, T. B. Marder, *Angew. Chem. Int. Ed.* **2014**, *53*, 1799–1803; *Angew. Chem.* **2014**, *126*, 1829–1834; c) T. Wang, D. W. Stephan, *Chem. Eur. J.* **2014**, *20*, 3036–3039; d) J. Lam, B. A. Günther, J. M. Farrell, P. Eisenberger, B. P. Bestvater, P. D. Newman, R. L. Melen, C. M. Crudden, D. W. Stephan, *Dalton Trans.* **2016**, *45*, 15303–15316; e) D. N. Lastovickova, C. W. Bielawski, *Organometallics* **2016**, *35*, 706–712; f) D. N. Lastovickova, C. W. Bielawski, *Catalysts* **2016**, *6*, 141; g) M. D. Anker, A. L. Colebatch, K. J. Iversen, D. J. D. Wilson, J. L. Dutton, L. García, M. S. Hill, D. J. Liptrot, M. F. Mahon, *Organometallics* **2017**, *36*, 1173–1178; h) M. Arrowsmith, J. Böhnke, H. Braunschweig, M. A. Celik, *Angew. Chem. Int. Ed.* **2017**, *56*, 14287–14292; *Angew. Chem.* **2017**, *129*, 14475–14480; i) B. Su, Y. Li, R. Ganguly, R. Kinjo, *Angew. Chem. Int. Ed.* **2017**, *56*, 14572–14576; *Angew. Chem.* **2017**, *129*, 14764–14768; j) J. J. Clarke, P. Eisenberger, S. S. Piotrkowski, C. M. Crudden, *Dalton Trans.* **2018**, *47*, 1791–1795; k) T. Brückner, M. Arrowsmith, M. Hess, K. Hammond, M. Müller, H. Braunschweig, *Chem. Commun.* **2019**, *55*, 6700–6703; l) D. Prieschl, M. Dietz, J. H. Muessig, K. Wagner, I. Krummenacher, H. Braunschweig, *Chem. Commun.* **2019**, *55*, 9781–9784; m) T. Thiess, S. K. Mellerup, H. Braunschweig, *Chem. Eur. J.* **2019**, *25*, 13572–13578; n) D. Prieschl, M. Arrowsmith, M. Dietz, A. Rempel, M. Müller, H. Braunschweig, *Chem. Commun.* **2020**, *56*, 5681–5684; o) L. Englert, U. Schmidt, M. Dömling, M. Passargus, T. E. Stennett, A. Hermann, M. Arrowsmith, M. Härterich, J. Müssig, A. Phillipps, D. Prieschl, A. Rempel, F. Röhm, K. Radacki, F. Schorr, T. Thiess, J. O. C. Jimenez-Halla, H. Braunschweig, *Chem. Sci.* **2021**, *12*, 9506–9515; p) Z. Guven, L. Denker, H. Dolati, D. Wullschlager, B. Trzaskowski, R. Frank, *Chem. Eur. J.* **2022**, *28*, e202200673; q) W. Lu, A. Jayaraman, F. Fantuzzi, R. D. Dewhurst, M. Härterich, M. Dietz, S. Hagspiel, I. Krummenacher, K. Hammond, J. Cui, H. Braunschweig, *Angew. Chem. Int. Ed.* **2022**, *61*, e202113947; *Angew. Chem.* **2022**, *134*, e202113947.

[9] K. J. Blakeney, P. D. Martin, C. H. Winter, *Organometallics* **2020**, *39*, 1006–1013.

[10] a) W. C. Chen, W. C. Shih, T. Jurca, L. Zhao, D. M. Andrada, C. J. Peng, C. C. Chang, S. K. Liu, Y. P. Wang, Y. S. Wen, G. P. A. Yap, C. P. Hsu, G. Frenking, T. G. Ong, *J. Am. Chem. Soc.* **2017**, *139*, 12830–12836; b) L. Garcia, K. H. M. Al Furaiji, D. J. D. Wilson, J. L. Dutton, M. S. Hill, M. F. Mahon, *Dalton Trans.* **2017**, *46*, 12015–12018.

[11] G. D. Frey, J. D. Masuda, B. Donnadieu, G. Bertrand, *Angew. Chem. Int. Ed.* **2010**, *49*, 9444–9447; *Angew. Chem.* **2010**,*122*, 9634–9637.

[12] a) H. Schneider, D. Schmidt, U. Radius, *Chem. Commun.* **2015**, *51*, 10138–10141; b) L. Werner, G. Horrer, M. Philipp, K. Lubitz, M. W. Kuntze-Fechner, U. Radius, *Z. Anorg. Allg. Chem.* **2021**, *647*, 881–895.

[13] a) G. D. Frey, V. Lavallo, B. Donnadieu, W. W. Schoeller, G. Bertrand, *Science* **2007**, *316*, 439–441; b) D. Martin, M. Soleilhavoup, G. Bertrand, *Chem. Sci.* **2011**, *2*, 389–399; c) M. M. D. Roy, A. A. Omana, A. S. S. Wilson, M. S. Hill, S. Aldridge, E. Rivard, *Chem. Rev.* **2021**, *121*, 12787–12965.

[14] C. P. Sindlinger, L. Wesemann, *Chem. Sci.* **2014**, *5*, 2739–2746.

[15] C. P. Sindlinger, S. Weiss, H. Schubert, L. Wesemann, *Angew. Chem. Int. Ed.* **2015**, *54*, 4087–4091; *Angew. Chem.* **2015**, *127*, 4160–4164.

[16] C. P. Sindlinger, L. Wesemann, *Chem. Commun.* **2015**, *51*, 11421–11424.

[17] C. P. Sindlinger, W. Grahneis, F. S. Aicher, L. Wesemann, *Chem. Eur. J.* **2016**, *22*, 7554–7566.

[18] J. J. Maudrich, C. P. Sindlinger, F. S. Aicher, K. Eichele, H. Schubert, L. Wesemann, *Chem. Eur. J.* **2017**, *23*, 2192–2200.

[19] M. Auer, F. Diab, K. Eichele, H. Schubert, L. Wesemann, *Dalton Trans.* **2022**, *51*, 5950–5961.

[20] a) Y. Xiong, T. Szilvasi, S. Yao, G. Tan, M. Driess, *J. Am. Chem. Soc.* **2014**, *136*, 11300–11303; b) K. Inomata, T. Watanabe, Y. Miyazaki, H. Tobita, *J. Am. Chem. Soc.* **2015**, *137*, 11935–11937; c) T. Fukuda, H. Hashimoto, H. Tobita, *J. Organomet. Chem.* **2017**, *848*, 89–94; d) J. A. Kelly, M. Juckel, T. J. Hadlington, I. Fernandez, G. Frenking, C. Jones, *Chem. Eur. J.* **2019**, *25*, 2773–2785; e) R. J. Mangan, A. Rit, C. P. Sindlinger, R. Tirfoin, J. Campos, J. Hicks, K. E. Christensen, H. Niu, S. Aldridge, *Chem. Eur. J.* **2020**, *26*, 306–315; f) R. J. Mangan, A. R. Davies, J. Hicks, C. P. Sindlinger, A. L. Thompson, S. Aldridge, *Polyhedron* **2021**, *196*, 115006.

[21] a) K. C. Thimer, S. M. Al-Rafia, M. J. Ferguson, R. McDonald, E. Rivard, *Chem. Commun.* **2009**, 7119–7121; b) S. M. Al-Rafia, A. C. Malcolm, S. K. Liew, M. J. Ferguson, R. McDonald, E. Rivard, *Chem. Commun.* **2011**, *47*, 6987–6989; c) S. M. Al-Rafia, A. C. Malcolm, S. K. Liew, M. J. Ferguson, E. Rivard, *J. Am. Chem. Soc.* **2011**, *133*, 777–779; d) I. S. M. Al-Rafia, P. A. Lummis, A. K. Swarnakar, K. C. Deutsch, M. J. Ferguson, R. McDonald, E. Rivard, *Aust. J. Chem.* **2013**, *66*, 1235–1245; e) S. M. Al-Rafia, M. R. Momeni, R. McDonald, M. J. Ferguson, A. Brown, E. Rivard, *Angew. Chem. Int. Ed.* **2013**, *52*, 6390–6395; *Angew. Chem.* **2013**, *125*, 6518–6523; f) S. M. I. Al-Rafia, M. R. Momeni, M. J. Ferguson, R. McDonald, A. Brown, E. Rivard, *Organometallics* **2013**, *32*, 6658–6665; g) M. M. D. Roy, S. Fujimori, M. J. Ferguson, R. McDonald, N. Tokitoh, E. Rivard, *Chem. Eur. J.* **2018**, *24*, 14392–14399; h) J. Sinclair, G. Dai, R. McDonald, M. J. Ferguson, A. Brown, E. Rivard, *Inorg. Chem.* **2020**, *59*, 10996–11008; i) M. Ackermann, M. Seidl, F. Wen, M. J. Ferguson, A. Y. Timoshkin, E. Rivard, M. Scheer, *Chem. Eur. J.* **2021**, *28*, e202103780.

[22] a) K. J. Iversen, D. J. Wilson, J. L. Dutton, *Dalton Trans.* **2013**, *42*, 11035–11038; b) K. J. Iversen, D. J. D. Wilson, J. L. Dutton, *Organometallics* **2013**, *32*, 6209–6217; c) M. R. Momeni, E. Rivard, A. Brown, *Organometallics* **2013**, *32*, 6201–6208; d) R. Fang, L. Z. Yang, Q. Wang, *Organometallics* **2014**, *33*, 53–60; e) K. J. Iversen, D. J. Wilson, J. L. Dutton, *Dalton Trans.* **2014**, *43*, 12820–12823; f) M. D. Su, *Inorg. Chem.* **2014**, *53*, 5080–5087; g) K. J. Iversen, D. J. Wilson, J. L. Dutton, *Dalton Trans.* **2015**, *44*, 3318–3325; h) K. J. Iversen, J. L. Dutton, D. J. D. Wilson, *Chem. Asian J.* **2017**, *12*, 1499–1508; i) K. H. M. Al Furaiji, K. J. Iversen, J. L. Dutton, D. J. D. Wilson, *Chem. Asian J.* **2018**, *13*, 3745–3752.

[23] J. A. Cooke, C. E. Dixon, M. R. Netherton, G. M. Kollegger, R. M. Baines, *Synth. React. Inorg. Met.-Org. Chem.* **1996**, *26*, 1205–1217.

[24] A. Castel, P. Riviere, J. Satge, H. Y. Ko, *Organometallics* **1990**, *9*, 205–210.

[25] A. J. Ruddy, P. A. Rupar, K. J. Bladek, C. J. Allan, J. C. Avery, K. M. Baines, *Organometallics* **2010**, *29*, 1362–1367.

[26] B. Watta, W. P. Neumann, J. Sauer, *Organometallics* **1985**, *4*, 1954–1957.

[27] a) B. Wrackmeyer in *Tin Chemistry: Fundamentals, Frontiers, and Apllications*, (Eds.: M. Gielen, A. G. Davies, K. Pannell, E. Tiekink), Wiley-VCH, Weinheim, **1996**, chapter 2; b) B. Wrackmeyer, U. Klaus, *J. Organomet. Chem.* **1996**, *520*, 211–226.

[28] a) T. Imori, V. Lu, H. Cai, T. D. Tilley, *J. Am. Chem. Soc.* **1995**, *117*, 9931–9940; b) V. Y. Lu, T. D. Tilley, *Macromolecules* **2000**, *33*, 2403–2412; c) F. Choffat, S. Käser, P. Wolfer, D. Schmid, R. Mezzenga, P. Smith, W. Caseri, *Macromolecules* **2007**, *40*, 7878–7889; d) D. Foucher in *Main Group Strategies towards Functional Hybrid Materials* (Eds.: H. Baumgartner, F. Jäkle), Wiley-VCH, Weinheim, **2018**, chapter 9.

Manuscript received: August 10, 2022
Accepted manuscript online: September 30, 2022
Version of record online: November 24, 2022